Published in final edited form as:
Dev Dyn. 2011 September ; 240(9): 2127–2141. doi:10.1002/dvdy.22702.

Transforming growth factor *Beta2* is required for valve remodeling during heart development

Mohamad Azhar[1,2,*], **Kristen Brown**[1], **Connie Gard**[1], **Hwudaurw Chen**[2], **Sudarsan Rajan**[3], **David A. Elliott**[2], **Mark V. Stevens**[4], **Todd D. Camenisch**[4,5,6], **Simon J. Conway**[7], and **Thomas Doetschman**[1,2]

[1]BIO5 Institute, University of Arizona, Tucson, AZ 85724

[2]Department of Cellular and Molecular Medicine, University of Arizona, Tucson, AZ 85724

[3]Department of Molecular Genetics, University of Cincinnati Collage of Medicine, OH

[4]Department of Pharmacology and Toxicology, University of Arizona, Tucson, AZ

[5]Steele Children's Research Center, University of Arizona, Tucson, AZ

[6]Southwest Environmental Health Sciences Center, University of Arizona, Tucson, AZ

[7]Developmental Biology and Neonatal Medicine Program, Herman B Wells Center for Pediatric Research, Indiana University School of Medicine, Indianapolis, IN 46202

Abstract

Although the function of transforming growth factor *beta*2 (TGFβ2) in epithelial mesenchymal transition (EMT) is well studied, its role in valve remodeling remains to be fully explored. Here, we used histological, morphometric, immunohistochemical and molecular approaches and showed that significant dysregulation of major extracellular matrix (ECM) components contributed to valve remodeling defects in *Tgfb2*$^{-/-}$ embryos. The data indicated that cushion mesenchymal cell differentiation was impaired in *Tgfb2*$^{-/-}$ embryos. Hyaluronan and cartilage link protein-1 (CRTL1) were increased in hyperplastic valves of *Tgfb2*$^{-/-}$ embryos, indicating increased expansion and diversification of cushion mesenchyme into the cartilage cell lineage during heart development. Finally, western blot and immunohistochemistry analyses indicate that the activation of SMAD2/3 was decreased in *Tgfb2*$^{-/-}$ embryos during valve remodeling. Collectively, the data indicate that TGFβ2 promotes valve remodeling and differentiation by inducing matrix organization and suppressing cushion mesenchyme differentiation into cartilage cell lineage during heart development.

Keywords

Transforming growth factor beta; valves; heart development

Introduction

Heart valve malformations are caused by defects in formation and remodeling of valves and are highly prevalent in patients of congenital heart disease (Supino et al. 2006;Lincoln and Yutzey 2011). Heart valve formation begins with an epithelial mesenchymal transition (EMT) at E9.5-E10.5 that forms the endocardial cushions in inflow or atrioventricular (AV)

[*]Correspondence to: Mohamad Azhar, 1656 E Mabel St, PO Box 245217, Tucson, AZ 85724-5217; azharm@email.arizona.edu.

Disclosures: None

and outflow tract (OFT) regions of the developing mouse heart (Delaughter et al. 2011). Endocardial cushions are the primordia of valves and septa and become mature structures through valve remodeling (E10.5-E18.5) (Person et al. 2005). Heart valve remodeling can be conceptually organized into multiple aspects, including mesenchymal expansion (E10.5-E12.5), differentiation (E12.5-E16.5), and condensation and maturation (E15.5-E18.5), all of which occur in an overlapping fashion (Markwald et al. 2010;Kruithof et al. 2007). During the maturation process the extracellular matrix (ECM) of inflow tract valves (tricuspid and mitral valves) or outflow tract valves (aortic and pulmonary valves) is organized into three distinct layers relative to blood flow: elastin-rich atrialis (inflow tract valves) or ventricularis (outflow tract valves), proteoglycan-rich spongiosa, and collagen-containing fibrosa (Wirrig and Yutzey 2011). This multilayer tissue organization of ECM not only provides structural integrity and resilience but it also regulates signal transduction pathways (Ng et al. 2004;Ramirez and Rifkin 2009). Although there are no strict time boundaries that separate multiple aspects of valvulogenesis, specific cellular and molecular characteristics are used to distinguish them (Abdelwahid et al. 2002;Hinton, Jr. et al. 2006;Lincoln et al. 2006a).

Transforming growth factor *beta* (TGFβ) ligands are multifunctional proteins that are involved in tissue development and homeostasis (Sporn and Roberts 1990;Derynck and Akhurst 2007). Although the role of TGFβ signaling in heart valve formation is well documented, the function of the three mammalian isoforms of TGFβ in valve remodeling is not fully understood (Mercado-Pimentel and Runyan 2007;Azhar et al. 2003;Arthur and Bamforth 2011). TGFβ ligands are produced as latent proteins and remain sequestered in an inactive form by several ECM proteins (Ramirez and Rifkin 2009). Following TGFβ ligand activation TGFβ usually interacts and forms a complex consisting of TGFβ type I receptor (TGFβR1, also known as ALK5) and TGFβ type II receptor (TGFβR2), sometimes in conjunction with either the Type III receptor (TGFβR3) or Endoglin, and can induce phosphorylation of TGFβ-specific SMADs (i.e., SMAD2/3) as well as Bone Morphogenetic Protein (BMP)-specific SMADs (i.e., SMAD1/5) (Daly et al. 2008;ten Dijke and Arthur 2007). TGFβR3 binds to TGFβ2 with a much higher affinity than it does to TGFβ1 or TGFβ3, and it is therefore thought that TGFβR3-TGFβ2 ligand-receptor pairing provides some specificity to TGFβ2 signaling (Brown et al. 1999). The phosphorylated or activated SMAD2/3 (pSMAD2/3) complex then in association with SMAD4 translocates to the nucleus and regulates gene transcription. Both TGFβ2 and BMP-2 are capable of stimulating the SMAD4 pathway (Townsend et al. 2011). SMAD7/6 act as antagonists of TGFβ/BMP signaling (Ross and Hill 2008;Tang et al. 2010). In addition, TGFβ1 can signal through ALK1 (BMP type I receptor) in endothelial cells (Arthur and Bamforth 2011). Furthermore, there are several other ways by which TGFβ signaling interacts with other important signal transduction pathways through SMAD-dependent or SMAD-independent mechanisms in order to regulate tissue development and homeostasis (Kang et al. 2009;Hoover et al. 2008;Li et al. 2010).

Some clarity for TGFβ ligand specificity in heart valve remodeling has been afforded by gene expression studies. In general, *Tgfb2* has high expression levels in cushion mesenchyme throughout valve development; whereas, *Tgfb3* expression occurs there only at later stages. *Tgfb1* is weakly expressed in cushion mesenchyme but strongly expressed in endocardium throughout valvulogenesis (Molin et al. 2003;Azhar et al. 2003;Vrljicak et al. 2009). Of the 3 different TGFβ ligand-deficient mice only *Tgfb2*$^{-/-}$ mice have congenital heart defects (Sanford et al. 1997;Proetzel et al. 1995;Kaartinen et al. 1995;Shull et al. 1992;Azhar et al. 2003). *Tgfb2*$^{-/-}$ mice exhibit multiple cardiovascular malformations with variable phenotypic penetrance. Some of the major cardiovascular anomalies include double-outlet right ventricle (DORV), ventricular septal defect (VSD), persistent truncus arteriosus (PTA), aortic arch artery malformations and abnormal cardiac cushions (Bartram et al. 2001;Azhar et al. 2009). We have previously shown that cardiac cushion formation

was defective in *Tgfb2*$^{-/-}$ embryos (Azhar et al. 2009;Bartram et al. 2001). However, the role of TGFβ2 in the post EMT endocardial cushion remodeling process has not been investigated.

In this study we determined the morphological, histological, cellular and molecular aspects that contributed to the remodeling defects in both inflow and outflow tract valves in the absence of TGFβ2. We reported these findings in the context of the associated cardiac malformations that were known to exist in the *Tgfb2*$^{-/-}$ mouse model. Comparison of cell proliferation (measured by *in vivo* BrdU incorporation), cell density and total cushion cell count in outflow and inflow tract valves during valve remodeling between wild-type and *Tgfb2*$^{-/-}$ embryos revealed defects in cushion mesenchymal cell differentiation in *Tgfb2*$^{-/-}$ embryos. Histochemistry and real time PCR analysis of *Tgfb2*$^{-/-}$ embryonic valves indicated altered expression of critical ECM components of valve structure. The data showed that CD34 that augmented valve differentiation in wild-type embryos was significantly reduced in the remodeling cushions of *Tgfb2*$^{-/-}$ embryos. The expression levels of hyaluronan and cartilage link protein-1 (CRTL1 or CLP) were elevated, which was consistent with excessive expansion and ectopic diversification of cushion mesenchyme into the cartilage cell lineage during valve remodeling in *Tgfb2*$^{-/-}$ embryos. Finally, canonical TGFβ signaling via SMAD2/3 was reduced during valve remodeling in *Tgfb2*$^{-/-}$ embryos. Since loss of TGFβ2 has similar effects on morphological, cellular and molecular aspects of the inflow and outflow tract valves, the conclusions are generalized to indicate that TGFβ2 plays similar roles in the remodeling of all valves. Combined, the data indicate novel and previously unidentified roles of TGFβ2 in valve remodeling during heart development.

Experimental Procedures

Mouse Strains

All procedures are approved by the Institutional Animal Care and Use the Committee at University of Arizona. *Tgfb2*$^{-/-}$ mice (129/Black-Swiss; 50:50 mix) were generated and genotyped as described (Sanford et al. 1997;Azhar et al. 2009). Embryos were collected between E10.5 and E18.5 and processed for histological and immunohistochemical, morphometric and molecular analyses as described (Azhar et al. 2009).

Histology and Morphometry

Hematoxylin and eosin staining was performed on 7 μm thick serial sections of heart for routine histological examination. Picrosirius Red (Garcia-Martinez et al. 1991), Weigert's Resorcin-Fuchsin (Zanetti et al. 2004), Alcian blue (pH2.5) (Snider et al. 2008) and Von Kossa (Peacock et al. 2010) staining was done on paraffin sections to detect valvular collagen fibers, elastin fibers, sulfated and non-sulfated glycosaminoglycans (GAGs) and calcification, respectively, in heart valves. To determine whether valves can be compared if mice are in different stages of the cardiac cycle, 70 μl of cold 0.5 M KCl (or 1×PBS control) was directly injected into the left ventricle of hearts of E16.5-E18.5 embryos to arrest them in diastole, as described (Kofler et al. 2004). Histological examination of heart valves was done by hematoxylin/eosin staining on serial sections of KCl-injected and 1× PBS-injected (randomly-arrested in systole or diastole at the time of death) control embryos. Morphometric measurements of combined total volume (mm^3) of the inflow and outflow tract cushions (hereafter termed total cushion volume) and combined total cell count in inflow and outflow tract cushions (hereafter termed total cushion cell count) were done as described (Bartram et al. 2001;Azhar et al. 2009). Briefly, the volumes of the cushion tissues were estimated according to Cavalieri (Gundersen and Jensen 1987;Bouman et al. 1997). Quantification of the total cushion cell count and cushion mesenchymal cells per area (μm^2) (also termed cell density) was done in 10 consecutive and corresponding hematoxylin/eosin-

stained tissue sections per embryo. All sections were visualized under bright-field optics with a Zeiss Axio Imager M1microscope (Carl Zeiss Microimaging, Inc., Thornwood, NY), and the morphometric measurements on the captured images were done by AxioVision 4.6.3 Zeiss imaging software. All experiments were done on more than 3 embryos per genotype per developmental stage with similar results.

Three dimensional reconstructions of heart valves

For 3-D valve reconstruction, digital images of 7 μm thick H&E stained serial sections were microscopically acquired and stacked with AutoAligner 2.0.0 (Bitplane AG, Minneapolis, MN). Photoshop 9 (Adobe, San Jose, CA) was used to identify and color-paint valvular structures as appropriate. Segmented images were then loaded into Volocity 3.1 (ImproVision Waltham, MA). Pixels had a known volume with the X & Y dimensions being determined from the resolution and magnification of the digital camera and the Z dimension being the thickness of the section. Volocity then calculated the volumes of structures of interest from at least three wild-type/mutant embryo pairs (Elliott et al. 2008).

Immunohistochemistry

Immunohistochemistry (IHC) was done on 4% paraformaldehyde-fixed 5 μm thick paraffin sections by using immunostaining kits (LSAB+ System-HRP (Cat #: K0690; CSA II Biotin-free Tyramide Signal Amplification System (Cat # K1497), according to the protocol of the manufacturer (DakoCytomation, CA), and as previously published (Azhar et al. 2009). Antigen retrieval was performed in Target Retrieval Solution pH 6.0 (Cat #: S1700; DakoCytomation, USA) for 15-20 minutes at 95°C. The following primary antibodies were used: muscle actin (Clone: HHF35, Cat # M0635; DakoCytomation) (1:50 dilution), CD34 (abcam, Cambridge, MA), CRTL1 (also called as hyaluronan and proteoglycan link protein 1 (HPLN1) (Developmental Hybridoma Bank, Iowa, MO), and phospho-SMAD2/3 (Chemicon, CA) (1:300). Immunostained sections were counterstained with nuclear stain hematoxylin. Hyaluronan was detected using biotinylated Hyaluronan-Binding Protein (HABP) (Seikagaku Corporation, catalog number 400763) as described previously (Wirrig et al. 2007). Alexa Fluor 568 secondary antibodies (A-11011 goat anti-rabbit IgG from Invitrogen, USA) were used for fluorescent detection of primary antibodies. For control staining, IgG isotype controls and/or preimmune serum (Pierce, IL) were used instead of the primary antibody. For quantification of hyaluronan levels in the valves the stain intensity was semiquantitatively graded to determine differences in HABP abundance in valves between wild-type and *Tgfb2*$^{-/-}$ embryos, as described (Evanko et al. 1998). The intensity of HABP staining from multiple images from embryos of both genotypes was graded on a scale from 0 to 3, with 0 indicating undetectable staining; 0.5, variably detectable staining; 1.0, detectable staining; 2.0, moderate staining; and 3.0, strong staining. Areas of measurement were restricted to the valves. More than three embryos per genotype were used for the analysis. The mean score was presented in histogram form. All stained sections (color or fluorescence) were analyzed using bright-field or fluorescence optics with a Zeiss Axio Imager M1 microscope (Carl Zeiss Microimaging, Inc., Thornwood, NY), and images were captured using AxioVision 4.6.3 imaging software.

Real time PCR analysis

Real time PCR was done on pooled cardiac tissue samples, which contained both inflow and outflow tract cushions. Cardiac tissue from wild-type or *Tgfb2*$^{-/-}$ embryos at E14.5 were microdissected under a stereozoom microscope and pooled from 3-6 embryos per sample per genotype. Total RNA from the pooled samples was isolated by RNeasy Mini kit (Cat # 74704: Qiagen, Valencia, CA). Three different pooled samples (representing a total of 9-18 embryos/genotype) of wild-type and *Tgfb2*$^{-/-}$ embryos were assessed by quantitative real time PCR, as described (Azhar et al. 2009). Each reaction was performed in triplicate. The

relative amount of target mRNA normalized to *Gapdh* was calculated according to the method described by Pfaffl (Pfaffl 2001). Specific primers that were used for the real time PCR amplification included (all sequences in 5′-3′ directions): *Fibrillin-1* forward, GGACGCCAATTTGGAGGCT; *Fibrillin-1* reverse, CTTTCAGCGCATCGTGTCCT; *Lysyl oxidase (Lox)* forward, TCTTCTGCTGCGTGACAACC; *Lox* reverse, GAGAAACCAGCTTGGAACCAG; versican (*Cspg2)* forward, ACTAACCCATGCACTACATCAAG; *Cspg2* reverse, ACTTTTCCAGACAGAGAGCCTT; hyaluronan-mediated motility receptor (*Rhamm*) forward, AGCAAAGCTCAATGCAGCAG; *Rhamm* reverse, AGTAAGCCGTTTTTCCAGTGAA; *CD34* forward, GGTAGCTCTCTGCCTGATGAG; *CD34* reverse, TGGTAGGAACTGATGGGGATATT; *Crtl1* forward, CCCCCGTCTACTTGTGGAAG; *Crtl1* reverse, TCCTGAGCCAAATGCTGTAGG; *Gapdh* forward, TGACCACAGTCCATGCCATC; *Gapdh* reverse, GACGGACACATTGGGGGTAG.

BrdU incorporation and quantification of cushion cell proliferation

Mouse embryos (E10.5 to E16.5) were labeled for 4 hr with 120 μg/gm body weight of BrdU labeling solution (Sigma), by means of an intraperitoneal injection into the body cavity of timed-pregnant mothers. Three wild-type and 3 $Tgfb2^{-/-}$ embryos were evaluated at each developmental stage by immunohistochemistry (IHC) using anti-BrdU antibody (Cat # B-2531; Sigma). Sections were counterstained with hematoxylin. About 20-30 consecutive and corresponding tissue sections per animal were scored to determine % of BrdU cushion cells and the total cushion cell count using bright-field optics with a Zeiss Axio Imager M1 microscope (Carl Zeiss Microimaging, Inc., Thornwood, NY) equipped with AxioVision 4.6.3 imaging software.

Western blot analysis

Microdissected cardiac tissue that contains the outflow and inflow tract cushions were pooled (4-6 embryos per genotype) from wild-type or $Tgfb2^{-/-}$ embryos at E14.5. Protein lysates were prepared from the pooled samples and tested by western blot as described (Azhar et al. 2009). Western blotting was performed in triplicate with similar results. Rabbit Phospho-SMAD2/3 (Ser465/467) (Cat # 3101; Cell Signaling Technology) (1:1000 dilution) was used to detect levels of pSMAD2/3. GRB2 (mouse anti-GRB2, BD Biosciences, Cat#610111) was used as a loading control, as described by others (Daly et al. 2008). Densitometry was done by using the program ONE-DScan (Scanalytics, VA, USA), and the ratio of pSMAD2/3 to GRB2 was calculated and plotted using SigmaPlot 11.0.

Statistical analysis

Data was reported as means ± S.E of the mean. Student's *t*-test (SigmaPlot, Systat Software, Inc., CA) was used for comparing groups. Significant differences were also probed using ANOVA. Pearson's chi-square test was used to find correlation between valve malformations and the associated malformations of the outflow tract, AV canal and aortic arch artery system. Microsoft Excel was used for managing the raw data. Probability values <0.05 were taken as significant. Probability values were shown on Figures wherever possible.

Results & Discussion

TGFβ2 is required for valve remodeling during heart development

The role of TGFβ2 in valve remodeling was carried out on E18.5 hearts at the histological, morphometric, immunohistochemical and expression levels. All embryos were analyzed for thickened outflow and/or inflow tract valves (N = 15 for wild-type embryos, N = 19 for

Tgfb2$^{-/-}$ embryos). The *Tgfb2*$^{-/-}$ embryos that displayed thickened valves were further characterized to determine the underlying developmental, cellular and molecular pathways involved in the valve remodeling defects. Thickening of the pulmonary, aortic, mitral and tricuspid valves was seen in both systole and diastole stages of the cardiac cycle (Fig. 1A-F). Histological examination of potassium chloride (KCl)-injected *Tgfb2*$^{-/-}$ embryos that were predominantly restricted in diastole also displayed significant valve thickening (not shown). It was not possible to specifically restrict embryos in systole. The effect of cardiac cycle on valve thickening in *Tgfb2*$^{-/-}$ embryos was determined because cardiac cyclic alteration in valvular thickness or length has been reported in age-related valve pathologies in humans (Mizushige et al. 1999;Brewer et al. 1977). Our results indicate that the stage of cardiac cycle has no effect on valve thickening in *Tgfb2*$^{-/-}$ embryos. Furthermore, the three dimensional valve reconstruction that confirmed mitral valve thickening in *Tgfb2*$^{-/-}$ embryos also revealed that chordae tendineae that are fibrous matrix structures that connect the mural leaflets of the mitral and tricuspid valves to papillary muscles were also abnormally thickened (Fig. 1G-H). Thickening of inflow and outflow tract valves in *Tgfb2*$^{-/-}$ embryos at E18.5 was quantified and confirmed by calculating the endocardial cushion volume [mm^3] according to the previously published method (Bartram et al. 2001). The data indicated that the volume of both the outflow tract valves (5.00e-3±5.75e-4 for wild-type vs. 0.02±2.02e-3 for *Tgfb2*$^{-/-}$, N = 5, P = 0.001) and the inflow tract valves (6.33e-3±1.20e-3 for wild-type vs. 0.02±2.40e-3 for *Tgfb2*$^{-/-}$, N = 5, P = 0.002) was higher in *Tgfb2*$^{-/-}$ embryos as compared to wild-type embryos at E18.5 (Fig. 1I,J). Together, the data indicate that *Tgfb2*$^{-/-}$ embryos at E18.5 exhibit thickening of both outflow and inflow tract valves.

We reported the findings on valve thickening in the context of the associated cardiac malformations that were known to exist in *Tgfb2*$^{-/-}$ embryos at E18.5 (Table 1-3). Of the13 cases of *Tgfb2*$^{-/-}$ embryos that were examined in this analysis, 4 embryos (30.7% cases) had thickened mitral valves, and 33.3% (4 out of 12 *Tgfb2*$^{-/-}$ embryos analyzed) had tricuspid valve thickening (Fig. 1E-H, Table 1). These data are consistent with our previously published findings (Bartram et al. 2001). However, of 11 cases of *Tgfb2*$^{-/-}$ embryos that were analyzed for outflow tract valve thickening, 9 (81.9%) showed thickened aortic valves, and 77.8% (7 out of 9 *Tgfb2*$^{-/-}$ embryos analyzed) showed thickened pulmonary valves (Fig. 1A-D, Table 1). In our previous study (Bartram et al. 2001) thickening of outflow tract valves was underestimated because it included only 3 *Tgfb2*$^{-/-}$ embryos at E18.5 of age that were combined in an E11.5-E18.5 developmental survey of cardiovascular phenotypes. The reason for this difference in frequency of valve thickening between outflow and inflow tract valves in *Tgfb2*$^{-/-}$ embryos remains unclear. The association between the thickened outflow and the thickened inflow tract valves was also investigated in *Tgfb2*$^{-/-}$ embryos at E18.5. The data indicate that there was no significant correlation of valve thickening between the outflow tract and inflow tract valves in *Tgfb2*$^{-/-}$ embryos ((P>0.05, Pearson's chi-square test) (Table 2). Collectively, these results indicate that valve thickening in outflow and inflow tract valves of *Tgfb2*$^{-/-}$ embryos is not inter-dependent.

Malformations of the outflow tract (DORV, common arterial trunk), AV canal (VSD, overriding tricuspid valves and complete AV septal defect), and aortic arch artery system (hypoplasia, interruption of the aortic arch, aberrant right subclavian artery and remnant of the right dorsal aorta) were also cataloged from all E18.5 *Tgfb2*$^{-/-}$ embryos that exhibited thickened valves. This was undertaken to determine if the abnormal valve thickening in *Tgfb2*$^{-/-}$ embryos was caused by the other cardiovascular malformations that were present in these embryos. This analysis found that *Tgfb2*$^{-/-}$ animals that had thickened valves always had some associated cardiovascular malformations ((P<0.05, Pearson's chi-square test) (Table 3). It is well documented that the outflow tract, AV canal and aortic arch artery abnormalities can occur both in the presence as well as absence of valve defects in various genetic mouse models of congenital heart disease (Moon 2008;Snider and Conway 2011).

The altered dimensions and molecular characteristics of the valves typically associated with the spectrum of heart defects seen in *Tgfb2*$^{-/-}$ mice have also been reported in other models of congenital heart disease. *Scleraxis* (*Scx*) null mice have thickened valvular structures without other structural defects in the developing cardiovascular system (Levay et al. 2008). By using a combination of conventional and conditional mouse genetics approaches it was shown that it is the deficiency of the neurofibromin gene (*Nf1*) and not the associated cardiovascular malformations that resulted in the enlarged valves in *Nf1*$^{-/-}$ mice (Lakkis and Epstein 1998;Gitler et al. 2003;Xu et al. 2009). Thus, it is reasonable to infer that the abnormal valve thickening in *Tgfb2*$^{-/-}$ embryos is primarily caused by loss of TGFβ2 and not the other cardiovascular malformations that are present in these embryos. However, in light of recent findings it is possible that the altered blood flow resulting from the defective septation found in *Tgfb2*$^{-/-}$ embryos could contribute to some aspects of their valve remodeling defects (Egorova et al. 2011). Collectively, the overall data indicate an important role of TGFβ2 in valve remodeling during heart development.

Decreased ECM organization during valve remodeling in TGFβ2-deficient embryos

Defects in ECM production, assembly and organization are found in enlarged diseased valves of mouse and human (Hinton and Yutzey 2011;Snider et al. 2008). Proteoglycans (i.e., glycosaminoglycans (GAGs), hyaluronan) and collagens, elastin, lysyl oxidase (LOX) and fibrillin-1 represent the major ECM components required for valve structure and function (Xu and Grande-Allen 2010;Hinton and Yutzey 2011;Wirrig and Yutzey 2011). By using different histological stains we found a severe disarray of ECM organization in the thickened outflow and inflow tract valves of *Tgfb2*$^{-/-}$ embryos. Weigert's Resorcin-Fuchsin staining for elastin at E18.5 indicated reduced elastin fibers in both the mitral and aortic valves of *Tgfb2*$^{-/-}$ embryos as compared to wild-type littermates (Fig. 2A-D, Supp Fig. S1A-B). For collagen fibers, Picrosirius Red-stained sections of E18.5 wild-type and *Tgfb2*$^{-/-}$ embryos were visualized using birefringent optics. The data showed a decreased distribution of collagen fibers in mitral and aortic valves and valve annulus of *Tgfb2*$^{-/-}$ embryos (Fig. 2E-F, Supp Fig. S1C-D). Histochemical examination by Von Kossa staining revealed no calcification in the thickened outflow or inflow tract valves of *Tgfb2*$^{-/-}$ embryos at E18.5 (not shown). Real time PCR analysis of pooled samples of cardiac tissue, which contained both inflow and outflow tract cushions, was done to measure *Fibrillin-1* and *Lox* message. Fibrillin-1 is an integral component of elastic fiber matrix and microfibrils (Ng et al. 2004). LOX crosslinks collagen with elastin and is essential for assembly of elastin-collagen fibers (Maki et al. 2002). Real time PCR analysis showed decreased *Fibrillin-1* and *Lox* message in valve-enriched cardiac tissue of *Tgfb2*$^{-/-}$ embryos (Fig. 2M). This, along with the reduced collagen and elastin fibers in *Tgfb2*$^{-/-}$ embryos, indicates reduced production, assembly and organization of ECM during valve remodeling in *Tgfb2*$^{-/-}$ embryos.

ECM components that constitute the spongiosa layer of the maturing valves were also investigated in *Tgfb2*$^{-/-}$ embryos. Proteoglycan-rich spongiosa predominantly consists of glycosaminoglycans (GAGs) and hyaluronan (Grande-Allen et al. 2007;Hinton and Yutzey 2011;Matsumoto et al. 2003). Hyaluronan is a unique non-sulfated GAG that is abundant during cushion formation, but its levels decrease during valve remodeling (Schroeder et al. 2003). Alcian blue staining was used to determine GAG levels in the thickened outflow and inflow tract valves of *Tgfb2*$^{-/-}$ embryos at E18.5. The data indicate significant overabundance of GAGs in the thickened mitral and aortic valves in *Tgfb2*$^{-/-}$ embryos (Fig. 2G-H, Supp Fig. S1E-F). These findings were reinforced by immunohistochemistry analysis of HABP in the thickened mitral valves of *Tgfb2*$^{-/-}$ embryos at E18.5. HABP is a known indicator of hyaluronan levels (Wirrig et al. 2007;Evanko et al. 1998). HABP staining intensity was semiquantitatively graded (see Experimental Procedures section for details) to determine differences in HABP abundance in the mitral valves between wild-type and

Tgfb2$^{-/-}$ embryos. Similar to the elevated GAGs levels in the mitral valves of *Tgfb2*$^{-/-}$ embryos, the data showed significantly increased deposition of hyaluronan in the thickened mitral valves of *Tgfb2*$^{-/-}$ embryos but not in wild-type embryos (Fig. 2I-K, Supp Fig. S1E-F). Real time PCR analysis of pooled samples of the cardiac tissue segment that contained both outflow tract and inflow tract cushions indicated that expression of versican (*Cspg2*) and the hyaluronan-mediated motility receptor (*Rhamm*) are significantly increased in *Tgfb2*$^{-/-}$ embryos (Fig. 2L). CSPG2 is coexpressed with hyaluronan in developing cushions and it biochemically interacts with hyaluronan (Matsumoto et al. 2003). In addition, mice heterozygous for *Cspg2* have reduced cushion volume supportive of this proteoglycan aggregate's functional connection in valvulogenesis (Kern et al. 2006;Wirrig et al. 2007;Matsumoto et al. 2003). RHAMM is an alternate receptor of hyaluronan (Amara et al. 1996). The real time PCR data also indicated no change in expression of the canonical hyaluronan receptor (CD44) (Schroeder et al. 2003) (not shown). The increased levels of hyaluronan and CSPG2 seem consistent with the elevated levels of CRTL1 (see below) and suggest an increased presence of proteoglycan aggregates in the valves of *Tgfb2*$^{-/-}$ embryos. Taken together, the results suggest that increased deposition of hyaluronan and its partner molecules along with significant overabundance of additional GAGs in valve spongiosa is involved in valve thickening in *Tgfb2*$^{-/-}$ embryos.

The data presented in this study demonstrate that valves of TGFβ2-deficient embryos at E18.5 exhibit characteristic changes that are seen in the ECM structure and organization of adult diseased valves of mouse and man, including reduced and irregular collagen-elastin fibers, and accumulation of GAGs and hyaluronan (Hinton and Yutzey 2011). Cardiac valve thickening caused by disrupted ECM organization is a common clinical manifestation of heart valve disease and one of the leading causes of valve insufficiency (Xu and Grande-Allen 2010;Charitakis and Basson 2007). Both hyaluronan and GAGs often serve as a sink for various crucial growth factors involved in valve formation and remodeling (Schroeder et al. 2003). Thus, higher levels of hyaluronan in cardiac valves of *Tgfb2*$^{-/-}$ embryos seem consistent with a heightened expansion of valve spongiosa, which in turn can contribute to improper maturation and valve thickening in *Tgfb2*$^{-/-}$ embryos. Elastin that makes up the atrialis/ventricularis is reduced in the thickened valves of *Tgfb2*$^{-/-}$ mice. Elastin is a major component of the valve structure, and its reduction has been shown to affect valve structure and function in adult mice (Hinton et al. 2010). Decreased collagen fibers are seen in the thickened valves of *Tgfb2*$^{-/-}$ embryos. Importantly, collagen deficiency can also cause valve thickening in mice (Lincoln et al. 2006b;Peacock et al. 2008). Collectively, our data indicate that a significant dysregulation in the composition and organization of critical ECM components is a major contributing factor for the valve remodeling defects in *Tgfb2*$^{-/-}$ embryos at E18.5. These findings are consistent with the notion that the foundation of the adult valve disease is rooted in abnormal valve development and remodeling. Further investigation is needed to determine whether TGFβ2 is also involved in valve homeostasis and valve disease in adulthood.

Impaired cushion mesenchyme differentiation in *Tgfb2*$^{-/-}$ embryos

Normal heart valve differentiation is characterized by reduced cell proliferation and increased apoptosis that result in reduced cushion volume of remodeling valve leaflets at E16.5 of gestation (Abdelwahid et al. 2002;Bartram et al. 2001;Lincoln et al. 2006a) A systematic analysis of cell proliferation using *in vivo* bromodeoxyuridine (BrdU) assays and total cell count in all cushions at different stages of valve development were done in both wild-type and *Tgfb2*$^{-/-}$ embryos (Fig. 3, Supp Fig. S2). Analysis of cells per area (μm^2) in outflow tract and inflow tract valves showed no significant change in cell density in *Tgfb2*$^{-/-}$ embryos (Fig. 3E). The cell proliferation as indicated by the % of BrdU cells was decreased in wild-types between E12.5 and E16.5 (P=0.0296, Student's *t*-test) (Fig. 3F). By contrast,

cell proliferation (Fig. 3F) and the total cell count in both outflow and inflow tract cushions (Fig. 3G) in *Tgfb2*$^{-/-}$ embryos were increased. In the absence of any significant change in cell density this observation was consistent with increased valve thickening in *Tgfb2*$^{-/-}$ embryos (Fig. 1A-F; Fig. 3A,C; Supp Fig. S2A,C). Importantly, the data also indicated that there was no difference in cell proliferation in *Tgfb2*$^{-/-}$ embryos between E10.5 and E12.5 stages when the valves were undergoing enormous cell proliferation (Fig. 3F) and expansion (Fig. 3G). Thus, these results indicate a defect in the valve differentiation program in *Tgfb2*$^{-/-}$ embryos, which is consistent with excess mesenchyme expansion rather than a higher proliferation rate of early mesenchyme. Morphometric measurement of the total endocardial cushion volume has previously established that a significant reduction in cushion volume at E14.5 in wild-type embryos is a reasonable indicator of valve differentiation status (Bartram et al. 2001). Delayed apoptosis also contributed to increased cushion cell counts in *Tgfb2*$^{-/-}$ embryos (Bartram et al. 2001). Since cardiac neural crest migration was apparently normal in *Tgfb2*$^{-/-}$ embryos (Gittenberger-de Groot et al. 2006), the data presented here indicate that impaired cushion differentiation into the valve lineage predominantly contributes to a sustained rise in cushion volume in the remodeling valves of *Tgfb2*$^{-/-}$ embryos.

Differentiating cushions condense the cushion matrix to form thinner fibrous valvular structures. Consequently, valve condensation, which involves significant cell-cell adhesion, results in increased cell density in valve leaflets as valves differentiate (Kruithof et al. 2007). Since cushion mesenchyme differentiation is impaired in *Tgfb2*$^{-/-}$ embryos, we have used CD34 as a molecular surrogate measure to determine the state of mesenchymal differentiation and condensation in these embryos. CD34 is a cluster of differentiation molecules present on early hematopoietic and vascular-associated tissues, including hematopoietic stem cell and cardiac endothelial progenitor cells and diseased valve interstitial cells (Krause et al. 1996;Visconti et al. 2006). It is a cell surface glycoprotein and functions as a differentiation factor and cell-cell adhesion molecule (Fackler et al. 1995;Traore and Hirn 1994). In wild-type mice, immunohistochemical staining showed that CD34 was highly expressed in remodeling cushion mesenchymes of both outflow tract and inflow tract valves (Fig. 4A,C,E). However, CD34 expression was decreased but remained detectable in the outflow and inflow tract valves of *Tgfb2*$^{-/-}$ embryos undergoing valve remodeling (Fig. 4B,D,F). This significant reduction in CD34 levels in valves of *Tgfb2*$^{-/-}$ embryos was confirmed by real time PCR of pooled samples of cardiac tissue, which contained both outflow tract and inflow tract cushions (Fig. 4G). Collectively, CD34 successfully marks differentiating, condensing and maturing valve mesenchyme of wild-type embryos, but its expression becomes low in thickened valves of *Tgfb2*$^{-/-}$ embryos. These findings are in agreement with previously reported observations showing that TGFβ signaling via a SMAD pathway induces CD34 expression in human hematopoietic primary stem/progenitor cells both at the transcriptional and protein levels (Pierelli et al. 2002). Furthermore, TGFβ2 has been shown to play an important role in the proliferation and repopulation capacity of hematopoietic stem cells (Avagyan et al. 2008). Intriguingly, published evidence indicates a role for CD34 in preventing the terminal differentiation of myeloid cells, and thus in maintaining the cells at an immature hematopoietic stage (Fackler et al. 1995). Since differentiation of cushion mesenchyme into the valve lineage is impaired in *Tgfb2*$^{-/-}$ embryos, this potential negative regulatory role for CD34 in cell differentiation seems consistent with the notion that instead of differentiating into valve mesenchyme, the cushion mesenchyme of *Tgfb2*$^{-/-}$ embryos differentiates into a non-valvular cell lineage. Indeed, further analysis indicated premature or ectopic differentiation and expansion of cushion mesenchyme into a cartilage cell lineage in *Tgfb2*$^{-/-}$ embryos (see below).

TGFβ2 is required for suppressing ectopic cartilage formation in developing heart valves

CRTL1 is a well known molecular marker of chondrogenic differentiation and cartilage formation (Lincoln et al. 2006a). CRTL1 is expressed in endocardially-derived cushion mesenchyme of outflow tract and inflow tract valves (Wirrig et al. 2007). CRTL1, hyaluronan and CSPG2 make up a proteoglycan aggregate in cartilage matrix (Matsumoto et al. 2003), and gene targeted ablation of *Crtl1* in mice results in decreased levels of hyaluronan and CSPG2 and severely underdeveloped cushions (Wirrig et al. 2007) Another study has shown that CRTL1 expression is increased in thickened valves of neonatal Scleraxis-deficient mice (Levay et al. 2008). Since *Tgfb2*$^{-/-}$ embryos have both thickened valves and increased hyaluronan and CSPG2, we determined the levels of CRTL1 by immunohistochemistry and its gene expression by real time PCR during valvulogenesis. In wild-type hearts, CRTL1 is expressed at considerable levels in pulmonary, aortic and tricuspid valves during heart development (Wirrig et al. 2007). However, there is no significant expression of CRTL1 in the mitral valves of the developing wild-type embryos (Wirrig et al. 2007). Immunohistochemistry data showed elevated levels of CRTL1 in pulmonary, aortic and tricuspid valves of *Tgfb2*$^{-/-}$ embryos (Fig. 5A-D). The CRTL1 levels were not significantly different in mitral valves between *Tgfb2*$^{-/-}$ and wild-type embryos (Fig. 5C-D). Real time PCR analysis of pooled samples of the cardiac tissue containing both outflow tract and inflow tract cushions also indicated increased expression of *Crtl1* in *Tgfb2*$^{-/-}$ embryos (Fig. 5E). Thus, the overall data indicate that CRTL1 is increased in all valves in *Tgfb2*$^{-/-}$ embryos where it is normally present in wild-type embryos.

The elevated CRTL1 levels in valves of *Tgfb2*$^{-/-}$ embryos are consistent with the elevated expression of both hyaluronan and CSPG2 in the thickened valves of these embryos. This is consistent with the known biochemical interaction of CRTL1, hyaluronan and CSPG2 levels in the cartilage matrix (Matsumoto et al. 2003). Valve mesenchymal cells are known to differentiate into chondrocytes (i.e., cartilage phenotype) or osteoblasts (i.e., bone phenotype) in heart valves during valve remodeling (Chakraborty et al. 2008;Lincoln et al. 2006a). Our data show that loss of TGFβ2 favors premature chondrogenic differentiation of cushion mesenchyme during valve remodeling in heart development. Published evidence indicates a role for CD34 in maintaining the cells at an immature stage (Fackler et al. 1995). CRTL1 is a well known molecular marker of chondrogenic differentiaton and cartilage formation in valves during heart development (Lincoln et al. 2006a). Since differentiation of cushion mesenchyme into the valve lineage is impaired in *Tgfb2*$^{-/-}$ embryos, this potential negative regulatory role for CD34 in cell differentiation and a positive connection of CRTL1 to cartilage lineage differentiation seems consistent with the notion that instead of differentiating into valve mesenchyme the cushion mesenchyme of *Tgfb2*$^{-/-}$ embryos prematurely differentiates into the cartilage cell lineage.

The observation that TGFβ2-deficiency promotes an ectopic cartilage cell lineage in aortic or tricuspid valves but not in mitral valves provides an important perspective to understanding the pathogenesis of valve diseases in adult humans. It has been shown that aortic valves, and rarely tricuspid valves, develop valve calcification and that the pathology of diseased mitral valves included myxomatous valve degeneration but not valve calcification (Caira et al. 2006). Of note, increased TGFβ signaling is consistent with osteogenic or calcific aortic valves in humans (Jian et al. 2003). It is also noteworthy that increased TGFβ signaling contributes to the myxomatous degeneration but not calcification of mitral valves (Ng et al. 2004). Hence, TGFβ regulation of the osteochondrogenic behavior of valve mesenchymal progenitor cells is crucial to an understanding of many heart valve diseases of adult humans. Whether TGFβ2 can directly and selectively regulate CRTL1 and suppress ectopic cartilage formation in developing heart valves remains to be determined, and unraveling this connection between these molecules in valvulogenesis will increase our understanding of the pathogenesis of adult human valve disease.

TGFβ2 is required for canonical TGFβ signaling pathway during valve remodeling

TGFβ ligand-dependent phosphorylation and activation of the TGFβ receptor complex is directly involved in phosphorylation and nuclear translocation of SMAD2/3 (pSMAD2/3) (Ross and Hill 2008). The level of pSMAD2/3 is considered a surrogate marker for canonical TGFβ signaling. Consequently, both immunohistochemistry (Fig. 6A-G) and western blot (Fig. 6H) methods were used to determine the levels of pSMAD2/3 in wild-type and *Tgfb2*$^{-/-}$ embryos during valvulogenesis. Western blot and subsequent densitometric analyses were used to quantify the levels of pSMAD2/3 in pooled samples of cardiac tissue containing both outflow and inflow tract cushions. The data showed that levels of pSMAD2/3 were decreased in remodeling cushion tissue of *Tgfb2*$^{-/-}$ embryos (Fig. 6H). This finding was further reinforced by immunohistochemistry analysis of the thickened valves of *Tgfb2*$^{-/-}$ embryos at E18.5. The data indicated that the percentage of pSMAD2/3-positive cells in the thickened inflow tract valves was decreased from 95.8% in wild-type embryos to 72.0% in *Tgfb2*$^{-/-}$ embryos (Fig. 6A-G). While most resident mesenchymal cells in the thickened inflow tract valves of *Tgfb2*$^{-/-}$ embryos retained sufficient phosphorylation of SMAD2/3, the mesenchymal cells with reduced pSMAD2/3 were sporadic (Fig. 6A-F, arrows). Interestingly, valve mesenchymal cells but not valve endothelium showed the most decrease in SMAD2/3 signaling (Fig. 6A-F, arrows). This is consistent with the known expression of *Tgfb2* in cushion mesenchyme during valve remodeling (Molin et al. 2003;Azhar et al. 2003). Overall, these results suggest that TGFβ2 is required for canonical pSMAD2/3-mediated TGFβ signaling during valve remodeling.

Reduced activation of SMAD2/3 in the thickened valves of *Tgfb2*$^{-/-}$ embryos is consistent with a recent finding indicating that reduced TGFβ2 and pSMAD2/3 activity contributes to valve thickening in the latent TGFβ binding protein-1 (*Ltbp1*$^{-/-}$) embryos (Todorovic et al. 2011). Moreover, the levels of the diphosphorylated ERK1/2 (dp-ERK) MAP kinase have been shown to be increased in the abnormal cushions of *Tgfb2*$^{-/-}$ embryos (Azhar et al. 2009). Collectively, TGFβ2 is required for maintaining a critical balance of both canonical (i.e., SMAD2/3-dependent) and non-canonical (SMAD-independent or ERK MAPK-mediated) TGFβ signaling pathways in valve remodeling during heart development. In contrast to the role of TGFβ2 signaling in embryonic valve development, increased *Tgfb2* expression and pSMAD2/3 levels are associated with the myxomatous degeneration and prolapse of mitral valves in adult *Fibrillin-1*$^{+/C1039G}$ mice (model of Marfan syndrome) (Ng et al. 2004). More importantly, recent studies have reported that mutations in TGFB2, TGFBR2 and SMAD3 cause cardiovascular complications, including valve malformations in humans (van, I et al. 2011;Shimizu et al. 2011). Thus, understanding the developmental, physiological and pathological functions of TGFβ2 has important clinical implications.

On a final note, in light of some recent findings it is speculated that in the absence of TGFβ2 a compensatory activated BMP2 signaling via TGFβR3 and ALK2 can contribute to abnormal cushion remodeling. These observations are based on the following observations. Firstly, it has been demonstrated that TGFβ2 and BMP2 acting through the TGFβR3 ligand(s)-receptor complex can regulate cushion formation (Townsend et al. 2011). Secondly, endothelial-specific deletion of ALK2, a BMP type 1 receptor, results in cushion remodeling defects associated with the downregulation of both pSMAD2/3 (TGFβ-specific SMADs) and pSMAD1/5/8 (BMP-specific SMADs) (Wang et al. 2005). Thirdly, it has been demonstrated that TGFβR2 and ALK5, as well as ALK2 and/or ALK3, are required for TGFβ-induced SMAD1/5 phosphorylation (Daly et al. 2008). It is also possible that TGFβ1 and/or TGFβ3 acting redundantly can signal through the TGFβ receptor complex in the absence of TGFβ2 and contribute to valve thickening (Arthur and Bamforth 2011). Thus, further investigation is required to determine whether a genetic interaction between *Tgfb2* and other TGFβ family ligands (i.e., *Tgfb1*,*Tgfb3*, *Bmp2*) or receptors (i.e., *Tgfbr3*, *Alk2*) is involved in valve formation, remodeling and homeostasis.

Conclusions

In summary, TGFβ2 is required for cushion remodeling and mature valve structure by promoting mesenchymal differentiation and condensation and ECM organization. TGFβ2 is also required for suppression of differentiation of cushion mesenchyme into a cartilage cell lineage during heart development. At the molecular level, CD34 and CRTL1 act as mediators of TGFβ2 function in valve remodeling. Finally, TGFβ2 is required for canonical TGFβ signaling during valve remodeling. Overall, the data show that TGFβ2 plays essential roles in valve remodeling during heart development. Understanding the mechanisms and signaling networks of TGFβ2 function in embryonic valve remodeling has implications for advancing congenital heart disease research.

Supplementary Material

Refer to Web version on PubMed Central for supplementary material.

Acknowledgments

We thank Cristopher Carney, Ilona Ormsby, and Eyad Nusayr for technical support and statistical data analysis. This work was supported, in parts, by funds from the National Institutes of Health Grants - HL070174 (TD), HL92508 (TD & SC), HL077493 (TC), HL82851-03 (RR), and HL105280 (DL). Additional funding was provided by Arizona Biomedical Research Commission (ABRC #0901) (MA) and The Stephen Michael Schneider/The William J. “Billy” Gieszl Award (MA).

Grant Sponsor: National Institutes of Health: HL92508 (TD & SC), HL070174 (TD), HL077493 (TC), HL82851 (RR), HL105280 (DL), Arizona Biomedical Research Commission: ABRC 0901 (MA); The Stephen Michael Schneider/The William J. “Billy” Gieszl Award (MA)

References

Abdelwahid E, Pelliniemi LJ, Jokinen E. Cell death and differentiation in the development of the endocardial cushion of the embryonic heart. Microsc Res Tech. 2002; 58:395–403. [PubMed: 12226809]

Amara FM, Entwistle J, Kuschak TI, Turley EA, Wright JA. Transforming growth factor-beta1 stimulates multiple protein interactions at a unique cis-element in the 3′-untranslated region of the hyaluronan receptor RHAMM mRNA. J Biol Chem. 1996; 271:15279–15284. [PubMed: 8663000]

Arthur HM, Bamforth SD. TGFbeta signaling and congenital heart disease: Insights from mouse studies. Birth Defects Res A Clin Mol Teratol. 2011:10.

Avagyan S, Glouchkova L, Choi J, Snoeck HW. A quantitative trait locus on chromosome 4 affects cycling of hematopoietic stem and progenitor cells through regulation of TGF-beta 2 responsiveness. J Immunol. 2008; 181:5904–5911. [PubMed: 18941179]

Azhar M, Runyan RB, Gard C, Sanford LP, Miller ML, Andringa A, Pawlowski S, Rajan S, Doetschman T. Ligand-specific function of transforming growth factor beta in epithelial-mesenchymal transition in heart development. Dev Dyn. 2009; 238:431–442. [PubMed: 19161227]

Azhar M, Schultz JE, Grupp I, Dorn GW, Meneton P, Molin DG, Gittenberger-de Groot AC, Doetschman T. Transforming growth factor beta in cardiovascular development and function. Cytokine Growth Factor Rev. 2003; 14:391–407. [PubMed: 12948523]

Bartram U, Molin DG, Wisse LJ, Mohamad A, Sanford LP, Doetschman T, Speer CP, Poelmann RE, Gittenberger-de GA. Double-outlet right ventricle and overriding tricuspid valve reflect disturbances of looping, myocardialization, endocardial cushion differentiation, and apoptosis in *Tgfb2* knockout mice. Circulation. 2001; 103:2745–2752. [PubMed: 11390347]

Bouman HG, Broekhuizen LA, Baasten AM, Gittenberger-de Groot AC, Wenink AC. Stereological study of stage 34 chicken hearts with looping disturbances after retinoic acid treatment: disturbed growth of myocardium and atrioventricular cushion tissue. Anat Rec. 1997; 248:242–250. [PubMed: 9185990]

Brewer RJ, Mentzer RM Jr, Deck JD, Ritter RC, Trefil JS, Nolan SP. An in vivo study of the dimensional changes of the aortic valve leaflets during the cardiac cycle. J Thorac Cardiovasc Surg. 1977; 74:645–650. [PubMed: 904366]

Brown CB, Boyer AS, Runyan RB, Barnett JV. Requirement of type III TGF-beta receptor for endocardial cell transformation in the heart. Science. 1999; 283:2080–2082. [PubMed: 10092230]

Caira FC, Stock SR, Gleason TG, McGee EC, Huang J, Bonow RO, Spelsberg TC, McCarthy PM, Rahimtoola SH, Rajamannan NM. Human degenerative valve disease is associated with up-regulation of low-density lipoprotein receptor-related protein 5 receptor-mediated bone formation. J Am Coll Cardiol. 2006; 47:1707–1712. [PubMed: 16631011]

Chakraborty S, Cheek J, Sakthivel B, Aronow BJ, Yutzey KE. Shared gene expression profiles in developing heart valves and osteoblast progenitor cells. Physiol Genomics. 2008

Charitakis K, Basson CT. Degenerating heart valves: fill them up with filamin? Circulation. 2007; 115:2–4. [PubMed: 17200451]

Daly AC, Randall RA, Hill CS. Transforming growth factor beta-induced Smad1/5 phosphorylation in epithelial cells is mediated by novel receptor complexes and is essential for anchorage-independent growth. Mol Cell Biol. 2008; 28:6889–6902. [PubMed: 18794361]

Delaughter DM, Saint-Jean L, Baldwin HS, Barnett JV. What chick and mouse models have taught us about the role of the endocardium in congenital heart disease. Birth Defects Res A Clin Mol Teratol. 2011:10.

Derynck R, Akhurst RJ. Differentiation plasticity regulated by TGF-beta family proteins in development and disease. Nat Cell Biol. 2007; 9:1000–1004. [PubMed: 17762890]

Egorova AD, Khedoe PP, Goumans MJ, Yoder BK, Nauli SM, ten Dijke P, Poelmann RE, Hierck BP. Lack of Primary Cilia Primes Shear-Induced Endothelial-to-Mesenchymal Transition. Circ Res. 2011; 108:1093–1101. [PubMed: 21393577]

Elliott DA, McIntosh MT, Hosgood HD III, Chen S, Zhang G, Baevova P, Joiner KA. Four distinct pathways of hemoglobin uptake in the malaria parasite Plasmodium falciparum. Proc Natl Acad Sci U S A. 2008; 105:2463–2468. [PubMed: 18263733]

Evanko SP, Raines EW, Ross R, Gold LI, Wight TN. Proteoglycan distribution in lesions of atherosclerosis depends on lesion severity, structural characteristics, and the proximity of platelet-derived growth factor and transforming growth factor-beta. Am J Pathol. 1998; 152:533–546. [PubMed: 9466580]

Fackler MJ, Krause DS, Smith OM, Civin CI, May WS. Full-length but not truncated CD34 inhibits hematopoietic cell differentiation of M1 cells. Blood. 1995; 85:3040–3047. [PubMed: 7538813]

Garcia-Martinez V, Sanchez-Quintana D, Hurle JM. Histochemical and ultrastructural changes in the extracellular matrix of the developing chick semilunar heart valves. Acta Anat (Basel). 1991; 142:87–96. [PubMed: 1781247]

Gitler AD, Zhu Y, Ismat FA, Lu MM, Yamauchi Y, Parada LF, Epstein JA. Nf1 has an essential role in endothelial cells. Nat Genet. 2003; 33:75–79. [PubMed: 12469121]

Gittenberger-de Groot AC, Azhar M, Molin DG. Transforming growth factor beta-SMAD2 signaling and aortic arch development. Trends Cardiovasc Med. 2006; 16:1–6. [PubMed: 16387623]

Grande-Allen KJ, Osman N, Ballinger ML, Dadlani H, Marasco S, Little PJ. Glycosaminoglycan synthesis and structure as targets for the prevention of calcific aortic valve disease. Cardiovasc Res. 2007; 76:19–28. [PubMed: 17560967]

Gundersen HJ, Jensen EB. The efficiency of systematic sampling in stereology and its prediction. J Microsc. 1987; 147:229–263. [PubMed: 3430576]

Hinton RB, Adelman-Brown J, Witt S, Krishnamurthy VK, Osinska H, Sakthivel B, James JF, Li DY, Narmoneva DA, Mecham RP, Benson DW. Elastin haploinsufficiency results in progressive aortic valve malformation and latent valve disease in a mouse model. Circ Res. 2010; 107:549–557. [PubMed: 20576933]

Hinton RB, Yutzey KE. Heart valve structure and function in development and disease. Annu Rev Physiol. 2011; 73:29–46. 29-46. [PubMed: 20809794]

Hinton RB Jr, Lincoln J, Deutsch GH, Osinska H, Manning PB, Benson DW, Yutzey KE. Extracellular matrix remodeling and organization in developing and diseased aortic valves. Circ Res. 2006; 98:1431–1438. [PubMed: 16645142]

Hoover LL, Burton EG, O'Neill ML, Brooks BA, Sreedharan S, Dawson NA, Kubalak SW. Retinoids regulate TGFbeta signaling at the level of Smad2 phosphorylation and nuclear accumulation. Biochim Biophys Acta. 2008; 1783:2279–2286. [PubMed: 18773928]

Jian B, Narula N, Li QY, Mohler ER III, Levy RJ. Progression of aortic valve stenosis: TGF-beta1 is present in calcified aortic valve cusps and promotes aortic valve interstitial cell calcification via apoptosis. Ann Thorac Surg. 2003; 75:457–465. [PubMed: 12607654]

Kaartinen V, Voncken JW, Shuler C, Warburton D, Bu D, Heisterkamp N, Groffen J. Abnormal lung development and cleft palate in mice lacking TGF-beta 3 indicates defects of epithelial-mesenchymal interaction. Nat Genet. 1995; 11:415–421. [PubMed: 7493022]

Kang JS, Liu C, Derynck R. New regulatory mechanisms of TGF-beta receptor function. Trends Cell Biol. 2009

Kern CB, Twal WO, Mjaatvedt CH, Fairey SE, Toole BP, Iruela-Arispe ML, Argraves WS. Proteolytic cleavage of versican during cardiac cushion morphogenesis. Dev Dyn. 2006; 235:2238–2247. [PubMed: 16691565]

Kofler J, Hattori K, Sawada M, DeVries AC, Martin LJ, Hurn PD, Traystman RJ. Histopathological and behavioral characterization of a novel model of cardiac arrest and cardiopulmonary resuscitation in mice. J Neurosci Methods. 2004; 136:33–44. [PubMed: 15126043]

Krause DS, Fackler MJ, Civin CI, May WS. CD34: structure, biology, and clinical utility. Blood. 1996; 87:1–13. [PubMed: 8547630]

Kruithof BP, Krawitz SA, Gaussin V. Atrioventricular valve development during late embryonic and postnatal stages involves condensation and extracellular matrix remodeling. Dev Biol. 2007; 302:208–217. [PubMed: 17054936]

Lakkis MM, Epstein JA. Neurofibromin modulation of ras activity is required for normal endocardial-mesenchymal transformation in the developing heart. Development. 1998; 125:4359–4367. [PubMed: 9778496]

Levay AK, Peacock JD, Lu Y, Koch M, Hinton RB Jr, Kadler KE, Lincoln J. Scleraxis is required for cell lineage differentiation and extracellular matrix remodeling during murine heart valve formation in vivo. Circ Res. 2008; 103:948–956. [PubMed: 18802027]

Li P, Pashmforoush M, Sucov HM. Retinoic acid regulates differentiation of the secondary heart field and TGFbeta-mediated outflow tract septation. Dev Cell. 2010; 18:480–485. [PubMed: 20230754]

Lincoln J, Florer JB, Deutsch GH, Wenstrup RJ, Yutzey KE. ColVa1 and ColXIa1 are required for myocardial morphogenesis and heart valve development. Dev Dyn. 2006b; 235:3295–3305. [PubMed: 17029294]

Lincoln J, Lange AW, Yutzey KE. Hearts and bones: shared regulatory mechanisms in heart valve, cartilage, tendon, and bone development. Dev Biol. 2006a; 294:292–302. [PubMed: 16643886]

Lincoln J, Yutzey KE. Molecular and developmental mechanisms of congenital heart valve disease. Birth Defects Res A Clin Mol Teratol. 2011:10.

Maki JM, Rasanen J, Tikkanen H, Sormunen R, Makikallio K, Kivirikko KI, Soininen R. Inactivation of the lysyl oxidase gene Lox leads to aortic aneurysms, cardiovascular dysfunction, and perinatal death in mice. Circulation. 2002; 106:2503–2509. [PubMed: 12417550]

Markwald RR, Norris RA, Moreno-Rodriguez R, Levine RA. Developmental basis of adult cardiovascular diseases: valvular heart diseases. Ann N Y Acad Sci. 2010; 1188:177–183. 177-83. [PubMed: 20201901]

Matsumoto K, Shionyu M, Go M, Shimizu K, Shinomura T, Kimata K, Watanabe H. Distinct interaction of versican/PG-M with hyaluronan and link protein. J Biol Chem. 2003; 278:41205–41212. [PubMed: 12888576]

Mercado-Pimentel ME, Runyan RB. Multiple transforming growth factor-beta isoforms and receptors function during epithelial-mesenchymal cell transformation in the embryonic heart. Cells Tissues Organs. 2007; 185:146–156. [PubMed: 17587820]

Mizushige K, Masugata H, Senda S, Manabe K, Sakamoto H, Kinoshita A, Sakamoto S, Matsuo H. Cyclic variation of thickness in an age-related thick mitral valve observed by transthoracic echocardiography. Angiology. 1999; 50:735–743. [PubMed: 10496500]

Molin DG, Bartram U, Van der HK, Van Iperen L, Speer CP, Hierck BP, Poelmann RE, Gittenberger-de-Groot AC. Expression patterns of Tgfbeta1-3 associate with myocardialisation of the outflow

tract and the development of the epicardium and the fibrous heart skeleton. Dev Dyn. 2003; 227:431–444. [PubMed: 12815630]

Moon A. Mouse models of congenital cardiovascular disease. Curr Top Dev Biol. 2008; 84:171–248. 171-248. [PubMed: 19186245]

Ng CM, Cheng A, Myers LA, Martinez-Murillo F, Jie C, Bedja D, Gabrielson KL, Hausladen JM, Mecham RP, Judge DP, Dietz HC. TGF-beta-dependent pathogenesis of mitral valve prolapse in a mouse model of Marfan syndrome. J Clin Invest. 2004; 114:1586–1592. [PubMed: 15546004]

Peacock JD, Levay AK, Gillaspie DB, Tao G, Lincoln J. Reduced sox9 function promotes heart valve calcification phenotypes in vivo. Circ Res. 2010; 106:712–719. [PubMed: 20056916]

Peacock JD, Lu Y, Koch M, Kadler KE, Lincoln J. Temporal and spatial expression of collagens during murine atrioventricular heart valve development and maintenance. Dev Dyn. 2008; 237:3051–3058. [PubMed: 18816857]

Person AD, Klewer SE, Runyan RB. Cell biology of cardiac cushion development. Int Rev Cytol. 2005; 243:287–335. 287-335. [PubMed: 15797462]

Pfaffl MW. A new mathematical model for relative quantification in real-time RT-PCR. Nucleic Acids Res. 2001; 29:e45. [PubMed: 11328886]

Pierelli L, Marone M, Bonanno G, Rutella S, de Ritis D, Mancuso S, Leone G, Scambia G. Transforming growth factor-beta1 causes transcriptional activation of CD34 and preserves haematopoietic stem/progenitor cell activity. Br J Haematol. 2002; 118:627–637. [PubMed: 12139758]

Proetzel G, Pawlowski SA, Wiles MV, Yin M, Boivin GP, Howles PN, Ding J, Ferguson MW, Doetschman T. Transforming growth factor-beta 3 is required for secondary palate fusion. Nat Genet. 1995; 11:409–414. [PubMed: 7493021]

Ramirez F, Rifkin DB. Extracellular microfibrils: contextual platforms for TGFbeta and BMP signaling. Curr Opin Cell Biol. 2009; 21:616–622. [PubMed: 19525102]

Ross S, Hill CS. How the Smads regulate transcription. Int J Biochem Cell Biol. 2008; 40:383–408. [PubMed: 18061509]

Sanford LP, Ormsby I, Gittenberger-de GA, Sariola H, Friedman R, Boivin GP, Cardell EL, Doetschman T. TGFbeta2 knockout mice have multiple developmental defects that are non-overlapping with other TGFbeta knockout phenotypes. Development. 1997; 124:2659–2670. [PubMed: 9217007]

Schroeder JA, Jackson LF, Lee DC, Camenisch TD. Form and function of developing heart valves: coordination by extracellular matrix and growth factor signaling. J Mol Med. 2003; 81:392–403. [PubMed: 12827270]

Shimizu C, Jain S, Davila S, Hibberd ML, Lin KO, Molkara D, Frazer JR, Sun S, Baker AL, Newburger JW, Rowley AH, Shulman ST, Davila S, Burgner D, Breunis WB, Kuijpers TW, Wright VJ, Levin M, Eleftherohorinou H, Coin L, Popper SJ, Relman DA, Fury W, Lin C, Mellis S, Tremoulet AH, Burns JC. Transforming Growth Factor-{beta} Signaling Pathway in Patients With Kawasaki Disease. Circ Cardiovasc Genet. 2011; 4:16–25. [PubMed: 21127203]

Shull MM, Ormsby I, Kier AB, Pawlowski S, Diebold RJ, Yin M, Allen R, Sidman C, Proetzel G, Calvin D, Doetschman T. Targeted disruption of the mouse transforming growth factor-beta 1 gene results in multifocal inflammatory disease. Nature. 1992; 359:693–699. [PubMed: 1436033]

Snider P, Conway SJ. Probing human cardiovascular congenital disease using transgenic mouse models. Prog Mol Biol Transl Sci. 2011; 100:83–110. 83-110. [PubMed: 21377625]

Snider P, Hinton RB, Moreno-Rodriguez RA, Wang J, Rogers R, Lindsley A, Li F, Ingram DA, Menick D, Field L, Firulli AB, Molkentin JD, Markwald R, Conway SJ. Periostin is required for maturation and extracellular matrix stabilization of noncardiomyocyte lineages of the heart. Circ Res. 2008; 102:752–760. [PubMed: 18296617]

Sporn MB, Roberts AB. TGF-beta: problems and prospects. Cell Regul. 1990; 1:875–882. [PubMed: 2100192]

Supino PG, Borer JS, Preibisz J, Bornstein A. The epidemiology of valvular heart disease: a growing public health problem. Heart Fail Clin. 2006; 2:379–393. [PubMed: 17448426]

Tang S, Snider P, Firulli AB, Conway SJ. Trigenic neural crest-restricted Smad7 over-expression results in congenital craniofacial and cardiovascular defects. Dev Biol. 2010

ten Dijke P, Arthur HM. Extracellular control of TGFbeta signalling in vascular development and disease. Nat Rev Mol Cell Biol. 2007

Todorovic V, Finnegan E, Freyer L, Zilberberg L, Ota M, Rifkin DB. Long form of latent TGF-beta binding protein 1 (Ltbp1L) regulates cardiac valve development. Dev Dyn. 2011; 240:176–187. [PubMed: 21181942]

Townsend TA, Robinson JY, Deig CR, Hill CR, Misfeldt A, Blobe GC, Barnett JV. BMP-2 and TGFbeta2 Shared Pathways Regulate Endocardial Cell Transformation. Cells Tissues Organs. 2011

Traore Y, Hirn J. Certain anti-CD34 monoclonal antibodies induce homotypic adhesion of leukemic cell lines in a CD18-dependent and a CD18-independent way. Eur J Immunol. 1994; 24:2304–2311. [PubMed: 7523134]

van dL I, Oldenburg RA, Pals G, Roos-Hesselink JW, de Graaf BM, Verhagen JM, Hoedemaekers YM, Willemsen R, Severijnen LA, Venselaar H, Vriend G, Pattynama PM, Collee M, Majoor-Krakauer D, Poldermans D, Frohn-Mulder IM, Micha D, Timmermans J, Hilhorst-Hofstee Y, Bierma-Zeinstra SM, Willems PJ, Kros JM, Oei EH, Oostra BA, Wessels MW, Bertoli-Avella AM. Mutations in SMAD3 cause a syndromic form of aortic aneurysms and dissections with early-onset osteoarthritis. Nat Genet. 2011; 43:121–126. [PubMed: 21217753]

Visconti RP, Ebihara Y, LaRue AC, Fleming PA, McQuinn TC, Masuya M, Minamiguchi H, Markwald RR, Ogawa M, Drake CJ. An in vivo analysis of hematopoietic stem cell potential: hematopoietic origin of cardiac valve interstitial cells. Circ Res. 2006; 98:690–696. [PubMed: 16456103]

Vrljicak PJ, Chang AC, Morozova O, Wederell ED, Niessen K, Marra MA, Karsan A, Hoodless PA. Genomic Analysis Distinguishes Phases of Early Development of the Mouse Atrio-Ventricular Canal. Physiol Genomics. 2009

Wang J, Sridurongrit S, Dudas M, Thomas P, Nagy A, Schneider MD, Epstein JA, Kaartinen V. Atrioventricular cushion transformation is mediated by ALK2 in the developing mouse heart. Dev Biol. 2005; 286:299–310. [PubMed: 16140292]

Wirrig EE, Snarr BS, Chintalapudi MR, O'neal JL, Phelps AL, Barth JL, Fresco VM, Kern CB, Mjaatvedt CH, Toole BP, Hoffman S, Trusk TC, Argraves WS, Wessels A. Cartilage link protein 1 (Crtl1), an extracellular matrix component playing an important role in heart development. Dev Biol. 2007; 310:291–303. [PubMed: 17822691]

Wirrig EE, Yutzey KE. Transcriptional regulation of heart valve development and disease. Cardiovasc Pathol. 2011; 20:162–167. [PubMed: 20705485]

Xu J, Ismat FA, Wang T, Lu MM, Antonucci N, Epstein JA. Cardiomyocyte-specific loss of neurofibromin promotes cardiac hypertrophy and dysfunction. Circ Res. 2009; 105:304–311. [PubMed: 19574548]

Xu S, Grande-Allen KJ. The role of cell biology and leaflet remodeling in the progression of heart valve disease. Methodist Debakey Cardiovasc J. 2010; 6:2–7. [PubMed: 20360651]

Zanetti M, Braghetta P, Sabatelli P, Mura I, Doliana R, Colombatti A, Volpin D, Bonaldo P, Bressan GM. EMILIN-1 deficiency induces elastogenesis and vascular cell defects. Mol Cell Biol. 2004; 24:638–650. [PubMed: 14701737]

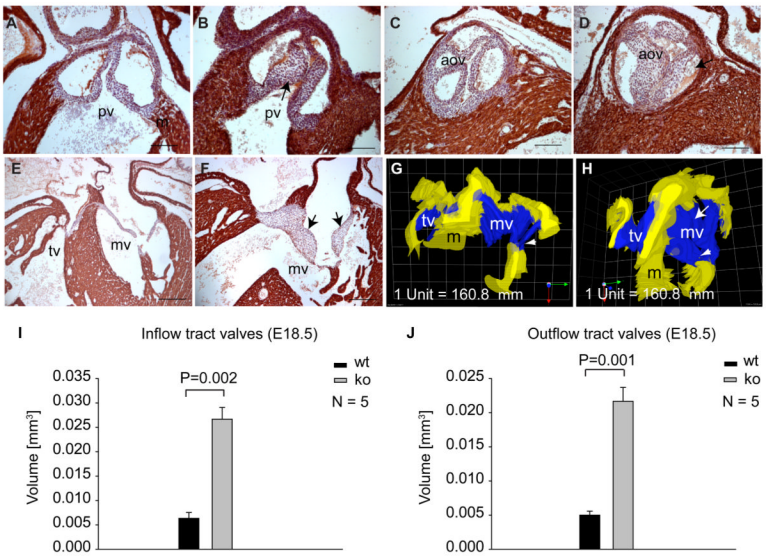

Fig. 1.

Cardiac valve thickening in *Tgfb2*$^{-/-}$ embryos. **A-F:** Immunohistochemistry showing cardiac valve morphology (HHF-35 staining for cardiac actin) in wild-type (A,C,E) and *Tgfb2*$^{-/-}$ (B,D,F) embryos at E18.5. Arrows denote thickened pulmonary (B), aortic (D) and mitral (F) valves in *Tgfb2*$^{-/-}$ embryos. **G,H:** Three-dimensional reconstructions of mitral valves of E18.5 wild-type and *Tgfb2*$^{-/-}$ embryos shown in (E and F) indicate leaflet thickening (arrow, H) and thickened chordae tendineae (arrowhead, H). Volume of the reconstructed mitral valves in *Tgfb2*$^{-/-}$ embryo (F,H) is 0.014 mm^3 and 0.004 mm^3 in wild-type embryo (E,G) All images (A-F) are representative of more than 9 wild-type/*Tgfb2*$^{-/-}$ embryo pairs. **I,J:** Morphometric comparison of inflow tract valves volume (I) and outflow tract valve volume between wild-type and *Tgfb2*$^{-/-}$ embryos at E18.5. Number of samples analyzed and the P values are given on the histograms. The total volume of inflow tract or outflow tract valves is significantly increased in *Tgfb2*$^{-/-}$ embryos as compared to wild-type embryos. Scale bar = 100 μm in (A-D), 200 μm (E,F). pv, pulmonary valves; aov, aortic valves; mv, mitral valves; m, myocardium; tv, tricuspid valves.

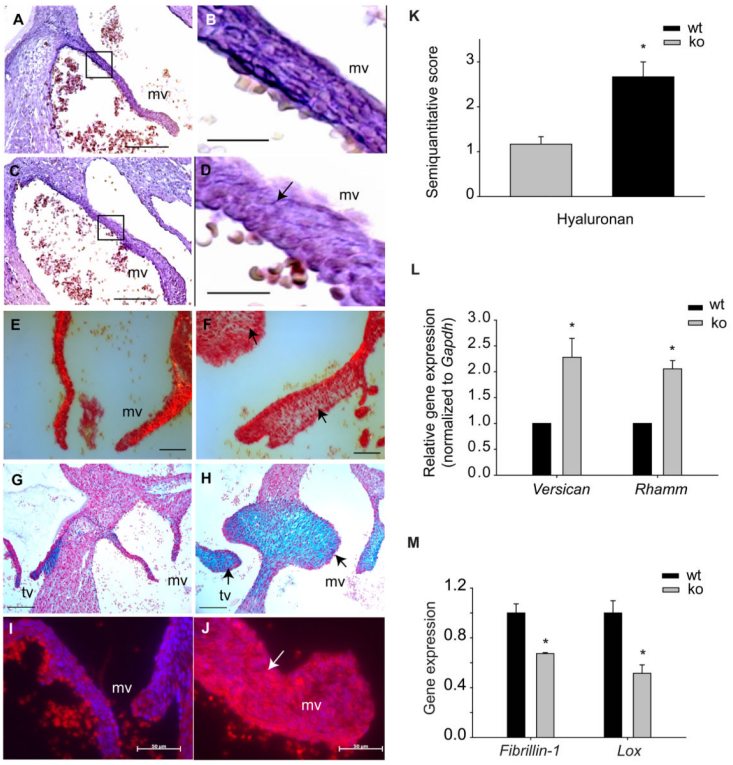

Fig. 2.

Dysregulated extracellular matrix organization in thickened valves of *Tgfb2*$^{-/-}$ embryos. **A-D:** Weigert's Resorcin-Fuchsin-staining of wild-type (A, B) and *Tgfb2*$^{-/-}$ (C, D) mitral valve leaflets at E18.5. Magnified views of regions indicated by the box in wild-type (A) and *Tgfb2*$^{-/-}$ (C) embryos are presented in (B) and (D), respectively, showing significantly decreased elastin fibers in *Tgfb2*$^{-/-}$ embryo compared to the wild-type embryo (D, arrow). **E-F:** Picrosirius Red-stained sections of wild-type (E) and *Tgfb2*$^{-/-}$ (F) embryos at E18.5 visualized in birefringent optics showing diffused collagen fibers in mitral valves of *Tgfb2*$^{-/-}$ embryos (arrows, F) as compared to wild-type embryo (E). **G,H:** Alcian blue staining showing excess accumulation of GAGs in inflow tract valves of *Tgfb2*$^{-/-}$ embryo (arrows in H) compared to the wild-type embryo (G) at E18.5. **I,J:** Immunohistochemistry indicating increased expression of HABP in mitral valves of *Tgfb2*$^{-/-}$ embryo (J) as compared to the wild-type embryo (I) at E18.5.**K:** Histogram showing the relative amount of hyaluronan in mitral valves as indicated by HABP florescence. The intensity of staining is graded semiquantitatively on a scale from 0 to 3, as described in details in Experimental Procedures section. The mean scores for mitral valves from more than three wild-type/*Tgfb2*$^{-/-}$ embryo pairs are presented. **L,M:** Real time PCR analyses on pooled cardiac tissue samples containing both outflow tract and inflow tract cushions of wild-type or *Tgfb2*$^{-/-}$ embryos at E14.5. Three biologically different pooled samples of wild-type and *Tgfb2*$^{-/-}$ embryos were assessed, as described in the Experimental Procedures. Each wild-type value is normalized to 1.0. The expression of *Cspg2* and the hyaluronan receptor *Rhamm* is significantly upregulated in *Tgfb2*$^{-/-}$ embryos compared to wild-type embryos at E14.5 (*P= 0.0248 for *Cspg2*, *P= 2.7484e-3 for *Rhamm*) (L). The expression of both *Fibrillin-1* (*P=0.0344) and *Lox* (*P=0.0154) is significantly reduced in *Tgfb2*$^{-/-}$ embryos as compared to wild-type embryos (M). All images (A-J) are representative of more than three wild-type/ *Tgfb2*$^{-/-}$ embryo pairs. Scale bar = 100 μm in (A, C), 20 μm (B, D), 50 μm in (E, F), 100 μm in (G,H), 50 μm in (I,J). wt, wild-type; ko, *Tgfb2*$^{-/-}$; mv, mitral valves.

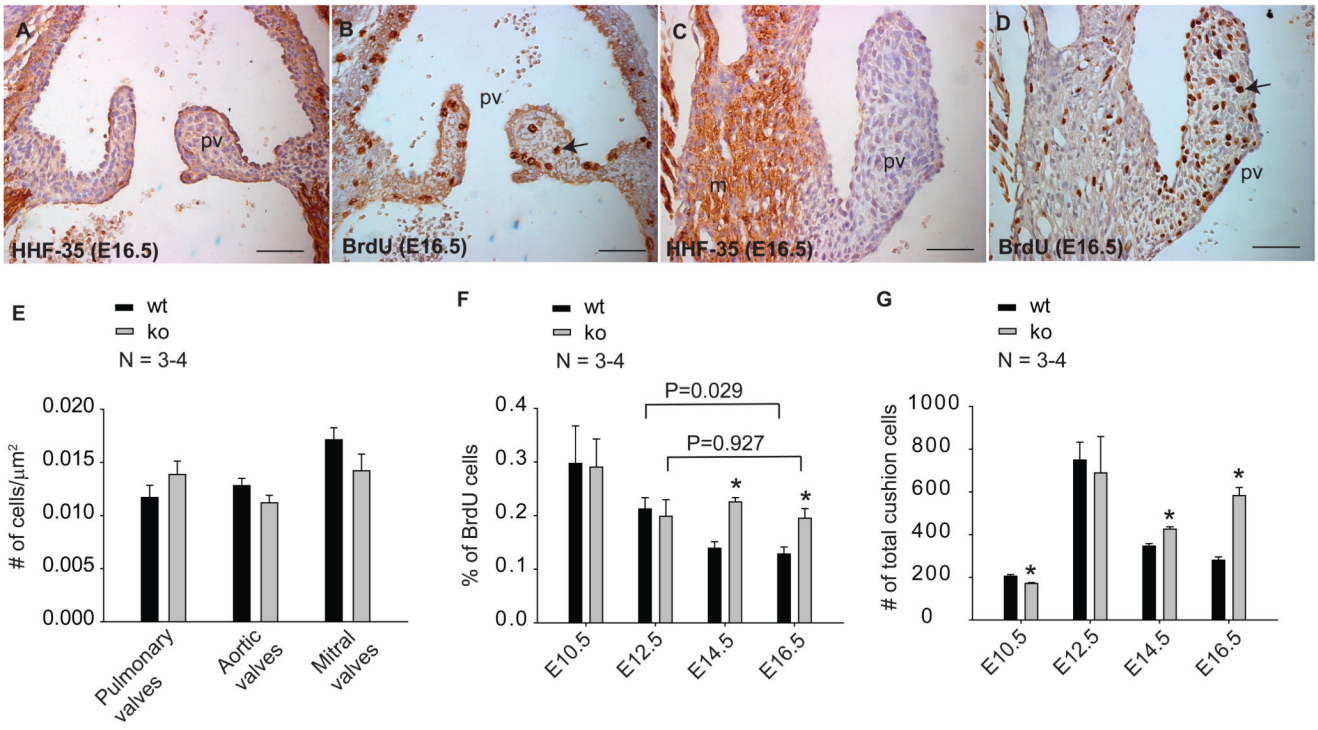

Fig. 3.

Impaired cushion cell differentiation in *Tgfb2*$^{-/-}$ embryos. **A-D:** Cardiac morphology (IHC: HHF-35, counterstained with hematoxylin) showing pulmonary valves in wild-type (A) and *Tgfb2*$^{-/-}$ (C) embryos and anti-BrdU-staining of their corresponding sections in wild-type (B) and *Tgfb2*$^{-/-}$ (D) embryos at E16.5. In (B,D), arrows indicate nuclear BrdU incorporating cells in pulmonary valves of developing hearts. All images (A-D) are representative of more than three wild-type/*Tgfb2*$^{-/-}$ embryo pairs. **E:** Morphometric comparison of cell density (# of cells/μm^2) (mean±s.e.m) in pulmonary, aortic and mitral valves of wild-type and *Tgfb2*$^{-/-}$ embryos at E16.5. There is no statistically significant difference in cell density in any valve types between wild-type and *Tgfb2*$^{-/-}$ embryos. **F:** % of BrdU incorporating cushion cells. Number of embryos per genotype analyzed and P values are given on the histogram. **G:** Total cell count in both outflow tract and inflow tract cushions in wild-types and *Tgfb2*$^{-/-}$ embryos showing that it is decreased at E10.5 (*P=0.0201), remains unchanged at E12.5 (P=0.7668) and increased at E14.5 (*P=7.6602e-3) and E16.5 (*P=1.7683e-3). Cell proliferation is comparable between wild-type and *Tgfb2*$^{-/-}$ cushions at E10.5 (P=0.9416) and E12.5 (P=0.9416) but the cell proliferation that is normally reduced in wild-type mice at E16.5 when compared with the wild-type at E12.5 (P=0.029) is not reduced in *Tgfb2*$^{-/-}$ embryos (P=0.0.927) (E), suggesting that impaired differentiation and not the cell proliferation of early cushion mesenchymal cells contribute to the increased expansion of cushion mesenchymal cells in *Tgfb2*$^{-/-}$ embryos. Scale bar = 50 μm in (A-D). pv, pulmonary valves; m, myocardium

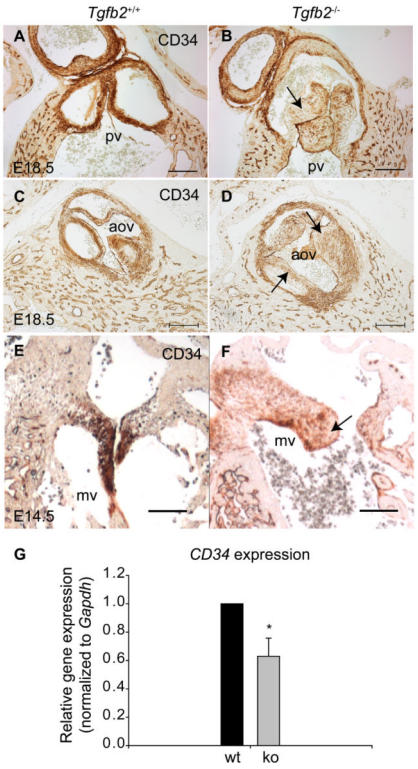

Fig. 4.

Reduced *CD34* expression during valvulogenesis in *Tgfb2*$^{-/-}$ embryos. **A-F:** Immunohistochemistry staining showing CD34 expression in pulmonary valves (A,B), aortic valves (C,D) and mitral valves (E,F) of wild-type (A,C,E) and *Tgfb2*$^{-/-}$ (B,D,F) embryos. Arrow in indicates low but detectable CD34 levels in the thickened pulmonary (B), aortic (D) and mitral (F) valves of *Tgfb2*$^{-/-}$ embryos. All images are representative of more than three wild-type/*Tgfb2*$^{-/-}$ embryo pairs. **G:** Real time PCR analysis to determine *CD34* expression in pooled cardiac tissue samples containing both outflow tract and inflow tract cushions from wild-type or *Tgfb2*$^{-/-}$ embryos at e14.5. Three biologically different pooled samples of wild-type or *Tgfb2*$^{-/-}$ embryos were assessed, as described in the Experimental Procedures. Each wild-type value is normalized to 1.0. *CD34* expression was significantly reduced in the remodeling cushions of *Tgfb2*$^{-/-}$ embryos as compared to wild-type embryos (*P=0.0277). Scale bar = 100 μm in (A-F). pv, pulmonary valves; aov, aortic valves; mv, mitral valves.

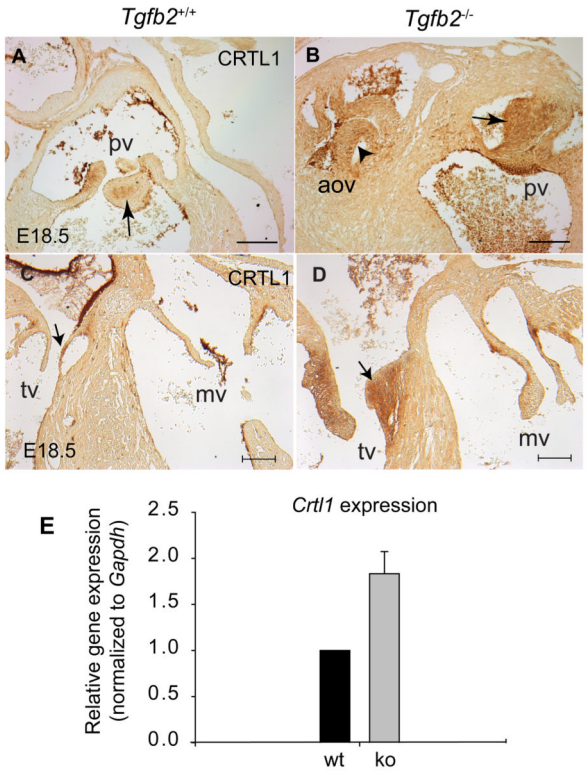

Fig. 5.

Ectopic cartilage differentiation during valve remodeling in *Tgfb2*$^{-/-}$ embryos. **A-D:** Immunohistochemistry staining showing protein levels of CRTL1 in outflow tract and inflow tract valves of wild-type (A,C) and *Tgfb2*$^{-/-}$ (B,D) embryos at E18.5. CRTL1 is restricted to a discrete population of valve mesenchymal cells (arrow, A) in maturing pulmonary valves of wild-type embryo. However, *Tgfb2*$^{-/-}$ embryo shows increased and ectopic levels of CRTL1 in both pulmonary (arrow, B) and aortic (arrowhead, B) valves. Note that in this *Tgfb2*$^{-/-}$ embryo (B) the pulmonary trunk and aorta are placed side-by-side and that this animal has a double-outlet right ventricle defect. Note that significant levels of CRTL1 are found in tricuspid valves (arrow, C) but not mitral valves in wild-type embryos. CRTL1 levels are increased in the thickened tricuspid valves of *Tgfb2*$^{-/-}$ embryo (arrow, D) as compared to wild-type embryos (C). CRTL1 levels are not different between wild-type and *Tgfb2*$^{-/-}$ embryos (C,D). All images are representative of more than three wild-type/ *Tgfb2*$^{-/-}$ embryo pairs. **E:** Confirmation of an upregulation of *Crtl1* gene expression by real time PCR analysis. The quantitative real time PCR is done in pooled cardiac tissue samples containing both outflow tract and inflow tract cushions from wild-type or *Tgfb2*$^{-/-}$ embryos at e14.5. Three biologically different pooled samples of wild-type or *Tgfb2*$^{-/-}$ embryos were assessed, as described in the Experimental Procedures. Each wild-type value is normalized to 1.0. *Crtl1* expression is increased during cushion remodeling in *Tgfb2*$^{-/-}$ embryos as compared to wild-type embryos (*P= 0.0257). Scale bar = 100 μm in (A-D). pv, pulmonary valves; aov, aortic valves; tv, tricuspid valves; mv, mitral valves.

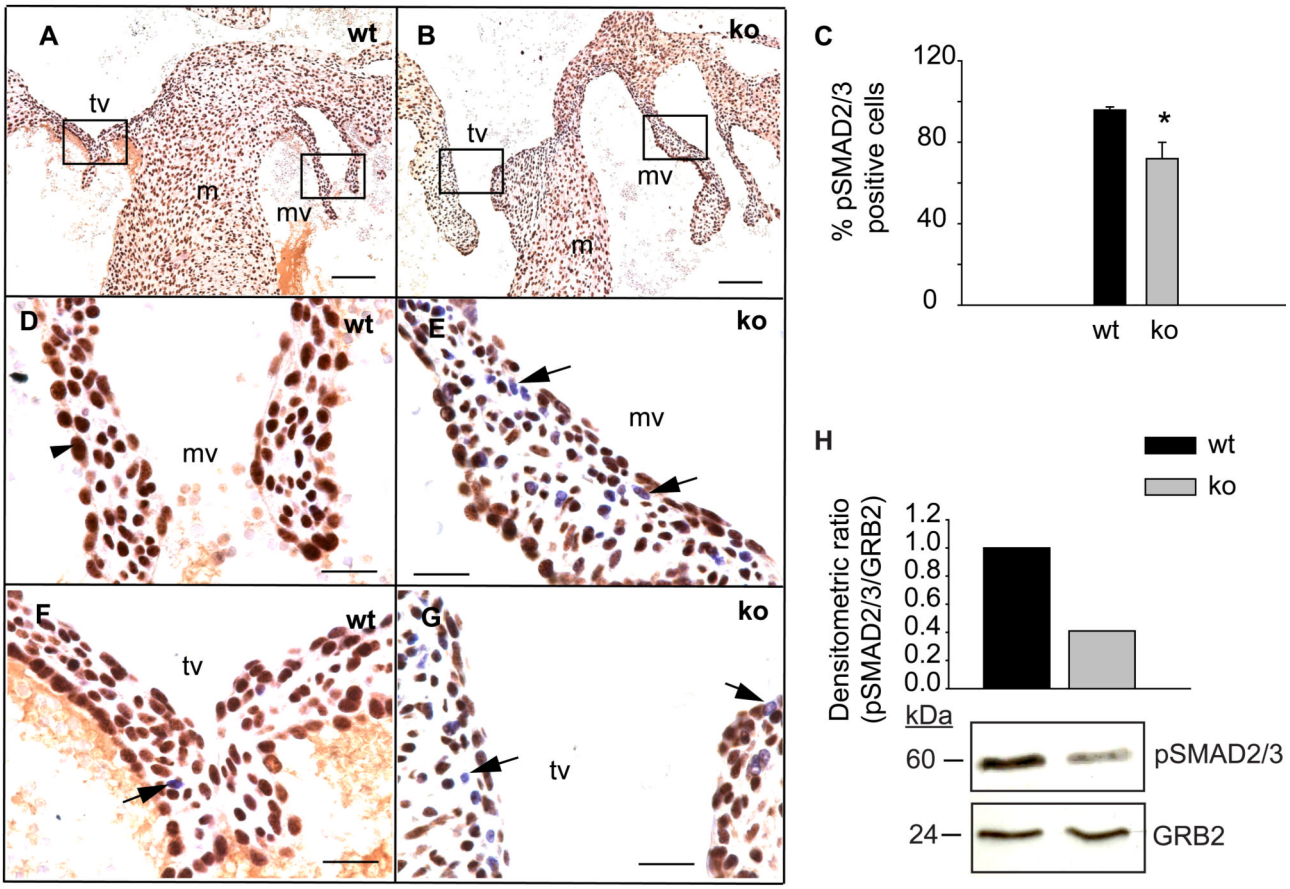

Fig. 6.

Reduced activation of SMAD2/3 during valve remodeling in *Tgfb2*$^{-/-}$ embryos. **A-G:** Immunohistochemistry staining showing pSMAD2/3 levels in thickened inflow tract valves of wild-type and *Tgfb2*$^{-/-}$ embryos at E18.5. The pSMAD2/3 staining in wild-type (A,D,F) and *Tgfb2*$^{-/-}$ (B,E,G) inflow tract valves is indicated by brown color. Boxes in (A) and (B) are magnified in (D,F) and (E,G), respectively. Reduction in pSMAD2/3 is indicated by increased visibility of hematoxylin counterstaining (blue or blue-brown color nuclei). Arrowhead in (D) indicates pSMAD2/3-positive cell and arrows in (F,E,G) denote cells with reduced pSMAD2/3. All images are representative of more than three wild-type/*Tgfb2*$^{-/-}$ embryo pairs. **C:** % of pSMAD2/3-positive cells is decreased in thickened mitral and tricuspid valves of the *Tgfb2*$^{-/-}$ embryos (*P=2.5186e-4). **H:** Representative western blot showing pSMAD2/3 levels in pooled samples of cardiac tissue containing outflow and inflow tract cushions (6 embryos per genotype) of wild-type and *Tgfb2*$^{-/-}$ embryos at E14.5 (see Experimental Procedures for details). GRB2 is used as the loading control. Histogram of densitometric ratio (pSMAD2/3/GRB2) is shown for a validation of the data presented in the western blot. Levels of pSMAD2/3 are downregulated in *Tgfb2*$^{-/-}$ embryos as compared to wild-types embryos during valve remodeling.

Scale: 100 μm in (A,B), 20 μm in (D,E,F,G). wt, wild-type; ko, *Tgfb2*$^{-/-}$; mv, mitral valves; m, myocardium; tv, tricuspid valves; pv, pulmonary valves.

Table 1

Cardiac valve thickening in *Tgfb2*$^{-/-}$ embryos at E18.5 (N = 14)

Thickened valve type	No. of cases analyzed	% of cases with thickened valves
Pulmonary valves	9	77.8
Aortic valves	11	81.8
Tricuspid valves	12	33.3
Mitral valves	13	30.7

Table 2

Association between thickened outflow tract and inflow tract valves in *Tgfb2*$^{-/-}$ embryos at E18.5 (N = 14)

Thickened valve type	Aortic valves	Tricuspid valves	Mitral valves
Pulmonary valves, n (%)	8 (87.5)	10 (40)	11 (27.2)
Aortic valves, n (%)	-	8 (50)	9 (22.2)

Table 3

Association of thickened valves to the malformations in other cardiovascular segments of *Tgfb2*$^{-/-}$ embryos at E18.5 (N = 14)

Thickened valve type	Outflow tract*	Inflow tract**	Aortic arch***
Pulmonary valves, n (%)	11 (90.9)	10 (90)	7 (85.7)
Aortic valves, n (%)	12 (91.6)	11 (81.8)	8 (87.5)
Tricuspid valves, n (%)	12 (41.6)	11 (36.3)	7 (42.8)
Mitral valves, n (%)	13 (30.7)	12 (33.3)	7 (14.2)

*Outflow tract malformations: DORV, common arterial trunk

**AV canal anomalies: Perimembranous inlet VSD, overriding of the tricuspid valves and complete AV septal defect

***Aortic arch artery abnormalities include: Hypoplasia of aortic arch, interruption of the aortic arch, aberrant right subclavian artery and remnant of right dorsal aorta